Search for Majorana Neutrinos in B[superscript –] → π[superscript +]μ[superscript –]μ[superscript –] Decays

Search for Majorana Neutrinos in $B^- \to \pi^+\mu^-\mu^-$ Decays

R. Aaij *et al.*[*]
(LHCb Collaboration)

(Received 21 January 2014; published 3 April 2014)

A search for heavy Majorana neutrinos produced in the $B^- \to \pi^+\mu^-\mu^-$ decay mode is performed using 3 fb^{-1} of integrated luminosity collected with the LHCb detector in pp collisions at center-of-mass energies of 7 and 8 TeV at the LHC. Neutrinos with masses in the range 250 to 5000 MeV and lifetimes from zero to 1000 ps are probed. In the absence of a signal, upper limits are set on the branching fraction $\mathcal{B}(B^- \to \pi^+\mu^-\mu^-)$ as functions of neutrino mass and lifetime. These limits are on the order of 10^{-9} for short neutrino lifetimes of 1 ps or less. Limits are also set on the coupling between the muon and a possible fourth-generation neutrino.

DOI: 10.1103/PhysRevLett.112.131802 PACS numbers: 13.35.Hb, 13.20.He, 14.40.Nd

Neutrinos can either be their own antiparticles, in which case they are called "Majorana" particles [1], or Dirac fermions. Heavy Majorana neutrinos can be sought in heavy flavor decays and couplings to a single fourth neutrino generation can be determined, or limits imposed, as in previous measurements [2,3]. The lepton number violating process $B^- \to \pi^+\mu^-\mu^-$, shown in Fig. 1, is forbidden in the standard model, but can proceed via the production of on-shell Majorana neutrinos. It is one of the most sensitive ways of looking for these particles in B meson decays, and has been modeled by Atre *et al.* [4]. Note that it is possible for virtual Majorana neutrinos of any mass to contribute to this decay. We investigate the $B^- \to \pi^+\mu^-\mu^-$ decay using 3 fb^{-1} of data acquired by the LHCb experiment in pp collisions. (In this Letter, mention of a particular decay implies the use of the charge-conjugate decay as well.) One-third of the data were recorded at 7 TeV center-of-mass energy, and the remainder at 8 TeV.

The search strategy is based on our previous analysis [2], but extends the sensitivity to neutrino lifetimes τ_N from the picosecond range up to about 1000 ps. The selection is aimed at maximizing the efficiency squared divided by the background yield. For lifetimes $\gtrsim$1 ps, the $\pi^+\mu^-$ decay products can appear as significantly detached from the B^- decay vertex. Therefore, we use two distinct strategies, one for short τ_N ($\mathcal{S}$) and another for τ_N up to 1000 ps ($\mathcal{L}$).

The LHCb detector is a single-arm forward spectrometer covering the pseudorapidity range $2 < \eta < 5$, designed for the study of particles containing b or c quarks [5]. The detector includes a high-precision tracking system consisting of a silicon-strip vertex detector surrounding the pp interaction region (VELO), a large-area silicon-strip detector located upstream of a dipole magnet with a bending power of about 4 Tm, and three stations of silicon-strip detectors and straw drift tubes placed downstream. The combined tracking system provides a momentum (p) measurement with relative uncertainty that varies from 0.4% at 5 GeV to 0.6% at 100 GeV. (We use natural units where $c = 1$.) The impact parameter is defined as the minimum track distance with respect to the primary vertex (PV). For tracks with large transverse momentum (p_T) with respect to the proton beam direction, the impact parameter resolution is approximately 20 μm. Charged hadrons are identified using two ring-imaging Cherenkov (RICH) detectors. Photon, electron, and hadron candidates are identified by a calorimeter system consisting of scintillating-pad and preshower detectors, an electromagnetic calorimeter, and a hadronic calorimeter. Muons are identified by a system composed of alternating layers of iron and multiwire proportional chambers.

The LHCb trigger [6] consists of a hardware stage, based on information from the calorimeter and muon systems, followed by a software stage that performs full event reconstruction. The hardware trigger selects either a single muon candidate with $p_T > 1.64$ GeV or two muons with the product of their p_T values being greater than 1.69 GeV^2. In the subsequent software stage, a muon candidate must form a vertex with one or two additional tracks that are detached from the PV. The trigger efficiency decreases for large lifetime Majorana neutrinos. Simulations are performed using PYTHIA [7], with the specific tuning given in Ref. [8], and the LHCb detector description based on GEANT [9] described in Ref. [10]. Decays of b hadrons are based on EVTGEN [11]. Simulation of $B^- \to \pi^+\mu^-\mu^-$ is carried out in two steps, the first being the two-body decay $B^- \to N\mu^-$, where N is a putative Majorana neutrino, and the second $N \to \pi^+\mu^-$.

[*] Full author list given at the end of the article.

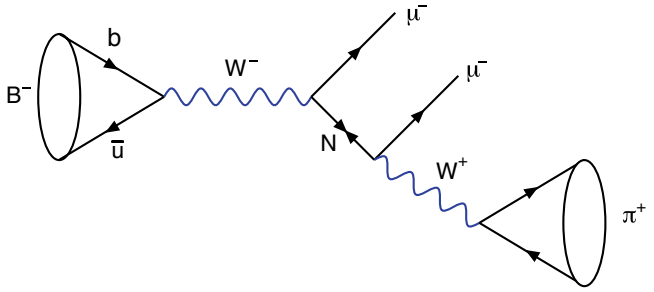

FIG. 1 (color online). Feynman diagram for $B^- \to \pi^+\mu^-\mu^-$ decay via a Majorana neutrino labeled N.

In both categories $\mathcal{S}$ and $\mathcal{L}$, only tracks that start in the VELO are used. We require muon candidates to have $p > 3$ GeV and $p_T > 0.75$ GeV, as muon detection provides fewer fakes above these values. The hadron must have $p > 2$ GeV and $p_T > 1.1$ GeV, in order to be tracked well. Muon candidate tracks are required to have hits in the muon chambers. The same criteria apply for the channel we use for normalization purposes, $B^- \to J/\psi K^-$ with $J/\psi \to \mu^+\mu^-$. Pion and kaon candidates must be positively identified in the RICH systems. For the $\mathcal{S}$ case and the normalization channel, candidate B^- combinations must form a common vertex with a χ^2 per number of degrees of freedom (ndf) less than 4. For the $\mathcal{L}$ candidates we require that the $\pi^+\mu^-$ tracks form a neutrino candidate (N) decay vertex with a $\chi^2 < 10$. A B^- candidate decay vertex is searched for by extrapolating the N trajectory back to a near approach with another μ^- candidate, which must form a vertex with the other muon having a $\chi^2 < 4$. The distance between the $\pi^+\mu^-$ and the primary vertex divided by its uncertainty must be greater than 10. The p_T of the $\pi^+\mu^-$ pair must also exceed 700 MeV. For both the $\mathcal{S}$ and $\mathcal{L}$ cases, we require that the cosine of the angle between the B^- candidate momentum vector and the line from the PV to the B^- vertex be greater than 0.99999. The two cases are not exclusive, with 16% of the event candidates appearing in both.

The mass spectra of the selected candidates are shown in Fig. 2. An extended unbinned likelihood fit is performed to the $J/\psi K^-$ mass spectrum with a double–Crystal Ball function [12] plus a triple-Gaussian background to account for partially reconstructed B decays and a linear function for combinatoric background. We find $282\,774 \pm 543$ signal events in the normalization channel. Backgrounds in the $\pi^+\mu^-\mu^-$ final state come from B decays to charmonium and combinatoric sources. Charmonium backgrounds are estimated using fully reconstructed $J/\psi K^-(\pi^-)$ and $\psi(2S)K^-(\pi^-)$ events and are indicated by shaded regions; they can peak at the B^- mass. No signal is observed in either the $\mathcal{S}$ or $\mathcal{L}$ samples.

We use the CL_s method to set upper limits [13], which requires the determination of the expected background yields and total number of events in the signal region. We define the signal region as the mass interval within $\pm 2\sigma$ of the B^- mass where σ is the mass resolution, specifically 5238.6–5319.8 MeV. Peaking background shapes and normalizations are fixed from exclusive reconstructions in the data. We fit the distributions outside of the B^- signal region with a sum of the peaking background tails, where both shape and normalization are fixed, and linear functions to account for the combinatorial backgrounds. The interpolated combinatoric background in each signal region is combined with the peaking background to determine the total background.

In the signal B mass range there are 19 events in the $\mathcal{S}$ sample and 60 events in the $\mathcal{L}$ sample. The $\mathcal{S}$ and $\mathcal{L}$ background fit yields are 17.8 ± 3.2 and 54.5 ± 5.4, respectively, in the same region.

The detection efficiency varies as a function of neutrino mass m_N, and changes for the $\mathcal{L}$ sample with τ_N. To quote an upper limit on the branching fraction for the $\mathcal{S}$ sample we take the average detection efficiency, as determined by simulation, with respect to the normalization mode of 0.687 ± 0.001. In computing the limit we include the uncertainties on background yields obtained from the fit to the $m(\pi^+\mu^-\mu^-)$ distribution and the systematic uncertainty described below. The normalization is obtained from the number of $J/\psi K^-$ events and the known rate of $\mathcal{B}(B^- \to J/\psi K^-, J/\psi \to \mu^+\mu^-) = (6.04 \pm 0.26) \times 10^{-5}$ [14,15]. We find

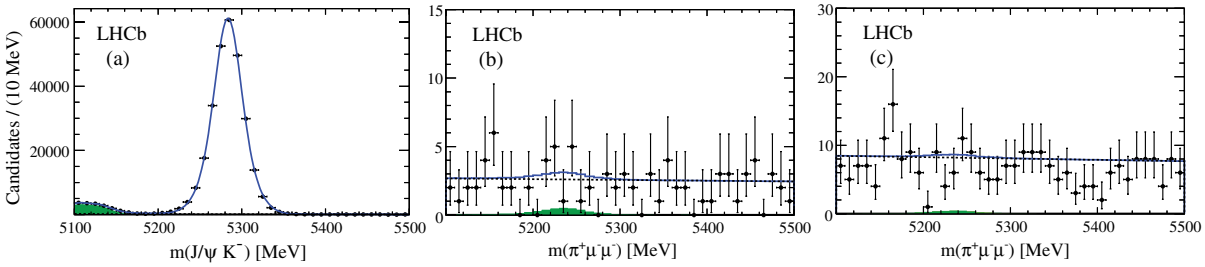

FIG. 2 (color online). Invariant mass distributions with fits overlaid of candidate mass spectra for (a) $J/\psi K^-$, (b) $\pi^+\mu^-\mu^-$ ($\mathcal{S}$), and (c) $\pi^+\mu^-\mu^-$ ($\mathcal{L}$). Backgrounds are (green) shaded; they peak under the signal in (b) and (c). The dotted lines show the combinatorial backgrounds only. The solid line shows the sum of both backgrounds.

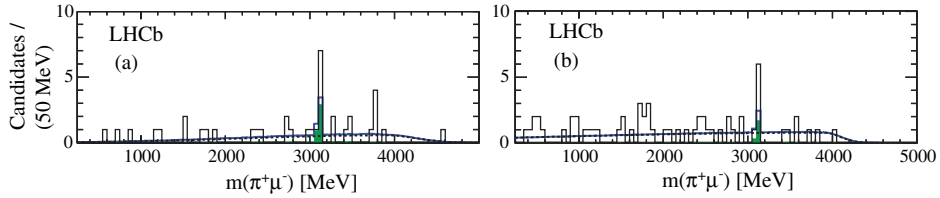

FIG. 3 (color online). Invariant $\pi^+\mu^-$ mass distribution for $\pi^+\mu^-\mu^-$ candidates with masses restricted to $\pm 2\sigma$ of B^- mass for the (a) $\mathcal{S}$ and (b) $\mathcal{L}$ selections. The shaded regions indicate the estimated peaking backgrounds. Backgrounds that peak under the signal in (a) and (b) are (green) shaded. The dotted lines show the combinatorial backgrounds only. The solid line is the sum of both backgrounds. [In (a) there are two combinations per event.]

$$\mathcal{B}(B^- \to \pi^+\mu^-\mu^-) < 4.0 \times 10^{-9}$$

at 95% confidence level.

This limit is applicable for $\tau_N \lesssim 1$ ps. The total systematic uncertainty is 6.6%. The largest source is $\mathcal{B}(B^- \to J/\psi K^-)$ (4.2%), followed by modeling of the efficiency ratio (3.5%) and backgrounds (3.5%), relative particle identification efficiencies (0.5%), tracking efficiency differences for kaons versus pions (0.5%), and yield of the normalization channel (0.4%).

We also search for signals as a function of m_N. The $\pi^+\mu^-$ mass spectra are shown in Fig. 3 for both $\mathcal{S}$ and $\mathcal{L}$ selections, requiring that the $\pi^+\mu^-\mu^-$ mass be restricted to the B^- signal range. There is an obvious peak around 3100 MeV from misidentified $J/\psi K^-$ (or π^-) events. The $\pi^+\mu^-$ mass spectra are fitted with a function derived from fitting the upper B^- sideband regions, from 5319.8 to 5400.0 MeV, for the combinatoric background, and peaking background components obtained from simulation.

As there is no evidence for a signal, upper limits are set by scanning across the m_N spectrum. At every 5 MeV step beginning at 250 MeV and ending at 5000 MeV we define a $\pm 3\sigma$ search region, where σ ranges from approximately 3 MeV at low mass to 24 MeV at high mass. The mass resolution is determined from fitting signals in other LHCb data [2]. The fitted background is then subtracted from the event yields in each interval. The upper limit at 95% C.L. of $\mathcal{B}(B^- \to \pi^+\mu^-\mu^-)$ at each mass value is computed using the CL_s method. The simulated efficiency ratio to the normalization mode averages about 0.8 up to 4000 MeV, and then approaching the phase space boundary, sharply decreases to 0.2 at 5000 MeV. The results of this scan are shown in Fig. 4.

The efficiency is highest for τ_N of a few ps, and decreases rapidly until about 200 ps when it levels off until about 1000 ps, beyond which it slowly vanishes as most of the decays occur outside of the vertex detector. For $\mathcal{L}$ candidates, we set upper limits as a function of both m_N and lifetime by performing the same scan in mass as before, but applying efficiencies appropriate for individual lifetime values between 1 and 1000 ps. The number of background events is extracted from the sum of combinatorial and peaking backgrounds in the fit to the $m(\pi^+\mu^-)$ distribution in the same manner as for the $\mathcal{S}$ sample. The estimated signal yield is the difference between the total number of events computed by counting the number in the interval and the fitted background yield. We take the τ_N dependence into account by using different efficiencies for each lifetime step. The two-dimensional plot of the upper limit on $\mathcal{B}(B^- \to \pi^+\mu^-\mu^-)$, computed using the CL_s method, is shown in Fig. 5.

Model-dependent upper limits on the coupling of a single fourth-generation Majorana neutrino to muons $|V_{\mu 4}|$ for each value of m_N are extracted using the formula from Atre *et al.* [4]:

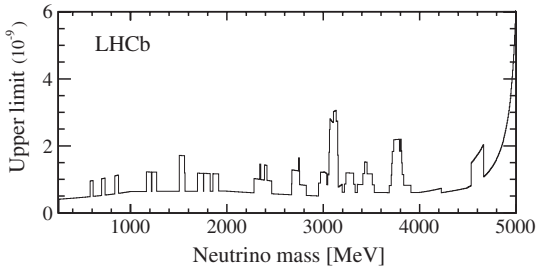

FIG. 4. Upper limit on $\mathcal{B}(B^- \to \pi^+\mu^-\mu^-)$ at 95% C.L. as a function of m_N in 5 MeV intervals for $\mathcal{S}$ selected events.

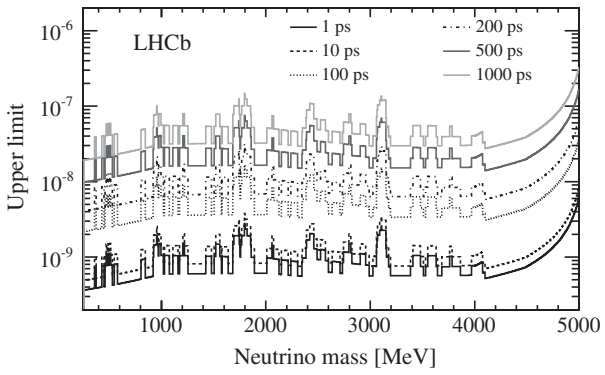

FIG. 5. Upper limits on $\mathcal{B}(B^- \to \pi^+\mu^-\mu^-)$ at 95% C.L. as a function of m_N, in 5 MeV intervals, for specific values of τ_N.

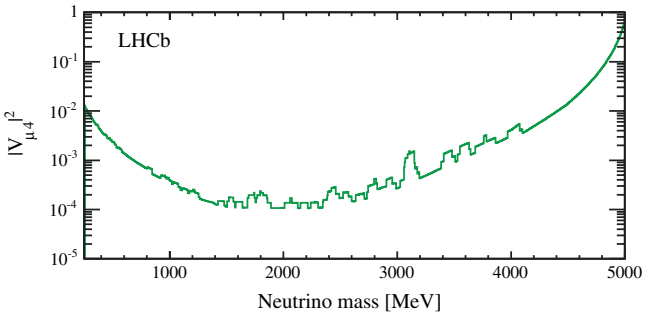

FIG. 6 (color online). Upper limits at 95% C.L. on $|V_{\mu 4}|^2$ are shown as a function of m_N for $\mathcal{L}$ events.

$$\mathcal{B}(B^- \to \pi^+\mu^-\mu^-) = \frac{G_F^4 f_B^2 f_\pi^2 m_B^5}{128\pi^2\hbar}|V_{ub}V_{ud}|^2\tau_B \times \left(1-\frac{m_N^2}{m_B^2}\right)\frac{m_N}{\Gamma_N}|V_{\mu 4}|^4, \quad (1)$$

with $G_F = 1.166377\times10^{-5}\,\mathrm{GeV}^{-2}$, $f_B = 0.19$ GeV, $f_\pi = 0.131$ GeV, $|V_{ub}| = 0.004$, $|V_{ud}| = 0.9738$, $m_B = 5.279$ GeV, $\tau_B = 1.671$ ps, and $\hbar = 6.582\times10^{-25}$ GeV s [15]. The total neutrino decay width Γ_N is a function of m_N and is proportional to $|V_{\mu 4}|^2$. In order to set limits on $|V_{\mu 4}|^2$, a model for Γ_N is required. The purely leptonic modes are specified in Ref. [4]. For the hadronic modes we use the fraction of times the charged current manifests itself as a single charged pion in τ^- and B^- decays, giving an additional m_N^3 dependent factor in Γ_N. The total width for Majorana neutrino decay is then

$$\Gamma_N = [3.95m_N^3 + 2.00m_N^5(1.44m_N^3 + 1.14)]\times10^{-13}|V_{\mu 4}|^2, \quad (2)$$

where m_N and Γ_N are in units of GeV. The first term corresponds to fully leptonic three-body decays, while the second is for decays into one lepton and hadrons.

To obtain upper limits on $|V_{\mu 4}|^2$ for each value of m_N we assume a value for $|V_{\mu 4}|$ and calculate Γ_N. This allows us to determine the τ_N dependent detection efficiency. We then use Eq. (1) to find the branching fraction. The value of $|V_{\mu 4}|$ is adjusted to match the previously determined upper limit value (see Fig. 5). The resulting 95% C.L. limit on $|V_{\mu 4}|^2$ is shown in Fig. 6 as a function of m_N. Limits have been derived by Atre *et al.* [4] for other experiments using different assumptions about the dependence of Γ_N with m_N, and thus cannot be directly compared. More searches exist for higher mass neutrinos [16]. The results presented here supersede previous LHCb results [2], significantly improve the limits on the $B^- \to \pi^+\mu^-\mu^-$ branching fraction, and extend the lifetime range of the Majorana neutrino search from a few picoseconds to 1 ns.

In conclusion, we have searched for on-shell Majorana neutrinos coupling to muons in the $B^- \to \pi^+\mu^-\mu^-$ decay channel as a function of m_N between 250 and 5000 MeV and for lifetimes up to ≈1000 ps. In the absence of a significant signal, we set upper limits on the $B^- \to \pi^+\mu^-\mu^-$ branching fraction and the coupling $|V_{\mu 4}|^2$ as a function of the neutrino mass.

We express our gratitude to our colleagues in the CERN accelerator departments for the excellent performance of the LHC. We thank the technical and administrative staff at the LHCb institutes. We acknowledge support from CERN and from the following national agencies: CAPES, CNPq, FAPERJ, and FINEP (Brazil); NSFC (China); CNRS/IN2P3 and Region Auvergne (France); BMBF, DFG, HGF, and MPG (Germany); SFI (Ireland); INFN (Italy); FOM and NWO (Netherlands); SCSR (Poland); MEN/IFA (Romania); MinES, Rosatom, RFBR, and NRC "Kurchatov Institute" (Russia); MinECo, XuntaGal, and GENCAT (Spain); SNSF and SER (Switzerland); NAS Ukraine (Ukraine); STFC (United Kingdom); NSF (U.S.). We also acknowledge the support received from the ERC under FP7. The Tier1 computing centers are supported by IN2P3 (France), KIT and BMBF (Germany), INFN (Italy), NWO and SURF (Netherlands), PIC (Spain), and GridPP (United Kingdom). We are indebted to the communities behind the multiple open source software packages we depend on. We are also thankful for the computing resources and the access to software R&D tools provided by Yandex LLC (Russia).

[1] E. Majorana, Nuovo Cimento **14**, 171 (1937).
[2] R. Aaij *et al.* (LHCb Collaboration), Phys. Rev. D **85**, 112004 (2012); Phys. Rev. Lett. **108**, 101601 (2012).
[3] J. P. Lees *et al.* (BABAR Collaboration), Phys. Rev. D **89**, 011102 (2014); O. Seon *et al.* (Belle Collaboration), Phys. Rev. D **84**, 071106 (2011); A. J. Weir *et al.* (MARK II Collaboration), Phys. Rev. D **41**, 1384 (1990).
[4] A. Atre, T. Han, S. Pascoli, and B. Zhang, J. High Energy Phys. 05 (2009) 030.
[5] A. A. Alves, Jr. *et al.* (LHCb Collaboration), JINST **3**, S08005 (2008).
[6] R. Aaij *et al.*, JINST **8**, P04022 (2013).
[7] T. Sjöstrand, S. Mrenna, and P. Z. Skands, J. High Energy Phys. 05 (2006) 026.
[8] I. Belyaev *et al.*, in *Proceedings of the IEEE Nuclear Science Symposium, 2010* (IEEE, New York, 2010), pp. 1155–1161.
[9] J. Allison *et al.* (GEANT4 Collaboration), IEEE Trans. Nucl. Sci. **53**, 270 (2006); S. Agostinelli *et al.* (GEANT4 Collaboration), Nucl. Instrum. Methods Phys. Res., Sect. A **506**, 250 (2003).
[10] M. Clemencic, G. Corti, S. Easo, C. R. Jones, S. Miglioranzi, M. Pappagallo, and P. Robbe, J. Phys. Conf. Ser. **331**, 032023 (2011).
[11] D. Lange, Nucl. Instrum. Methods Phys. Res., Sect. A **462**, 152 (2001).

[12] T. Skwarnicki, Ph.D. thesis, Institute of Nuclear Physics, Krakow, 1986 [DESY Report No. DESY-F31-86-02].
[13] T. Junk, Nucl. Instrum. Methods Phys. Res., Sect. A **434**, 435 (1999).
[14] R. Aaij *et al.* (LHCb Collaboration), Phys. Rev. D **87**, 072004 (2013).
[15] J. Beringer *et al.* (Particle Data Group), Phys. Rev. D **86**, 010001 (2012), and 2013 partial update for the 2014 edition.
[16] S. Chatrchyan *et al.* (CMS Collaboration), Phys. Lett. B **717**, 109 (2012); G. Aad *et al.* (ATLAS Collaboration), J. High Energy Phys. 1110 (2011) 107; Eur. Phys. J. C **72**, 2056 (2012).

R. Aaij,[40] B. Adeva,[36] M. Adinolfi,[45] A. Affolder,[51] Z. Ajaltouni,[5] J. Albrecht,[9] F. Alessio,[37] M. Alexander,[50] S. Ali,[40] G. Alkhazov,[29] P. Alvarez Cartelle,[36] A. A. Alves Jr.,[24] S. Amato,[2] S. Amerio,[21] Y. Amhis,[7] L. Anderlini,[17,g] J. Anderson,[39] R. Andreassen,[56] M. Andreotti,[16,f] J. E. Andrews,[57] R. B. Appleby,[53] O. Aquines Gutierrez,[10] F. Archilli,[37] A. Artamonov,[34] M. Artuso,[58] E. Aslanides,[6] G. Auriemma,[24,n] M. Baalouch,[5] S. Bachmann,[11] J. J. Back,[47] A. Badalov,[35] V. Balagura,[30] W. Baldini,[16] R. J. Barlow,[53] C. Barschel,[38] S. Barsuk,[7] W. Barter,[46] V. Batozskaya,[27] T. Bauer,[40] A. Bay,[38] J. Beddow,[50] F. Bedeschi,[22] I. Bediaga,[1] S. Belogurov,[30] K. Belous,[34] I. Belyaev,[30] E. Ben-Haim,[8] G. Bencivenni,[18] S. Benson,[49] J. Benton,[45] A. Berezhnoy,[31] R. Bernet,[39] M.-O. Bettler,[46] M. van Beuzekom,[40] A. Bien,[11] S. Bifani,[44] T. Bird,[53] A. Bizzeti,[17,i] P. M. Bjørnstad,[53] T. Blake,[47] F. Blanc,[38] J. Blouw,[10] S. Blusk,[58] V. Bocci,[24] A. Bondar,[33] N. Bondar,[29] W. Bonivento,[15,37] S. Borghi,[53] A. Borgia,[58] M. Borsato,[7] T. J. V. Bowcock,[51] E. Bowen,[39] C. Bozzi,[16] T. Brambach,[9] J. van den Brand,[41] J. Bressieux,[38] D. Brett,[53] M. Britsch,[10] T. Britton,[58] N. H. Brook,[45] H. Brown,[51] A. Bursche,[39] G. Busetto,[21,r] J. Buytaert,[37] S. Cadeddu,[15] R. Calabrese,[16,f] O. Callot,[7] M. Calvi,[20,k] M. Calvo Gomez,[35,p] A. Camboni,[35] P. Campana,[18,37] D. Campora Perez,[37] A. Carbone,[14,d] G. Carboni,[23,l] R. Cardinale,[19,j] A. Cardini,[15] H. Carranza-Mejia,[49] L. Carson,[49] K. Carvalho Akiba,[2] G. Casse,[51] L. Castillo Garcia,[37] M. Cattaneo,[37] C. Cauet,[9] R. Cenci,[57] M. Charles,[8] P. Charpentier,[37] S.-F. Cheung,[54] N. Chiapolini,[39] M. Chrzaszcz,[39,25] K. Ciba,[37] X. Cid Vidal,[37] G. Ciezarek,[52] P. E. L. Clarke,[49] M. Clemencic,[37] H. V. Cliff,[46] J. Closier,[37] C. Coca,[28] V. Coco,[37] J. Cogan,[6] E. Cogneras,[5] P. Collins,[37] A. Comerma-Montells,[35] A. Contu,[15,37] A. Cook,[45] M. Coombes,[45] S. Coquereau,[8] G. Corti,[37] I. Counts,[55] B. Couturier,[37] G. A. Cowan,[49] D. C. Craik,[47] M. Cruz Torres,[59] S. Cunliffe,[52] R. Currie,[49] C. D'Ambrosio,[37] J. Dalseno,[45] P. David,[8] P. N. Y. David,[40] A. Davis,[56] I. De Bonis,[4] K. De Bruyn,[40] S. De Capua,[53] M. De Cian,[11] J. M. De Miranda,[1] L. De Paula,[2] W. De Silva,[56] P. De Simone,[18] D. Decamp,[4] M. Deckenhoff,[9] L. Del Buono,[8] N. Déléage,[4] D. Derkach,[54] O. Deschamps,[5] F. Dettori,[41] A. Di Canto,[11] H. Dijkstra,[37] S. Donleavy,[51] F. Dordei,[11] M. Dorigo,[38] P. Dorosz,[25,o] A. Dosil Suárez,[36] D. Dossett,[47] A. Dovbnya,[42] F. Dupertuis,[38] P. Durante,[37] R. Dzhelyadin,[34] A. Dziurda,[25] A. Dzyuba,[29] S. Easo,[48] U. Egede,[52] V. Egorychev,[30] S. Eidelman,[33] S. Eisenhardt,[49] U. Eitschberger,[9] R. Ekelhof,[9] L. Eklund,[50,37] I. El Rifai,[5] C. Elsasser,[39] A. Falabella,[16,f] C. Färber,[11] C. Farinelli,[40] S. Farry,[51] D. Ferguson,[49] V. Fernandez Albor,[36] F. Ferreira Rodrigues,[1] M. Ferro-Luzzi,[37] S. Filippov,[32] M. Fiore,[16,f] M. Fiorini,[16,f] C. Fitzpatrick,[37] M. Fontana,[10] F. Fontanelli,[19,j] R. Forty,[37] O. Francisco,[2] M. Frank,[37] C. Frei,[37] M. Frosini,[17,37,g] E. Furfaro,[23,l] A. Gallas Torreira,[36] D. Galli,[14,d] M. Gandelman,[2] P. Gandini,[58] Y. Gao,[3] J. Garofoli,[58] J. Garra Tico,[46] L. Garrido,[35] C. Gaspar,[37] R. Gauld,[54] E. Gersabeck,[11] M. Gersabeck,[53] T. Gershon,[47] P. Ghez,[4] A. Gianelle,[21] V. Gibson,[46] L. Giubega,[28] V. V. Gligorov,[37] C. Göbel,[59] D. Golubkov,[30] A. Golutvin,[52,30,37] A. Gomes,[1,a] H. Gordon,[37] M. Grabalosa Gándara,[5] R. Graciani Diaz,[35] L. A. Granado Cardoso,[37] E. Graugés,[35] G. Graziani,[17] A. Grecu,[28] E. Greening,[54] S. Gregson,[46] P. Griffith,[44] L. Grillo,[11] O. Grünberg,[60] B. Gui,[58] E. Gushchin,[32] Y. Guz,[34,37] T. Gys,[37] C. Hadjivasiliou,[58] G. Haefeli,[38] C. Haen,[37] T. W. Hafkenscheid,[62] S. C. Haines,[46] S. Hall,[52] B. Hamilton,[57] T. Hampson,[45] S. Hansmann-Menzemer,[11] N. Harnew,[54] S. T. Harnew,[45] J. Harrison,[53] T. Hartmann,[60] J. He,[37] T. Head,[37] V. Heijne,[40] K. Hennessy,[51] P. Henrard,[5] J. A. Hernando Morata,[36] E. van Herwijnen,[37] M. Heß,[60] A. Hicheur,[1] D. Hill,[54] M. Hoballah,[5] C. Hombach,[53] W. Hulsbergen,[40] P. Hunt,[54] T. Huse,[51] N. Hussain,[54] D. Hutchcroft,[51] D. Hynds,[50] V. Iakovenko,[43] M. Idzik,[26] P. Ilten,[55] R. Jacobsson,[37] A. Jaeger,[11] E. Jans,[40] P. Jaton,[38] A. Jawahery,[57] F. Jing,[3] M. John,[54] D. Johnson,[54] C. R. Jones,[46] C. Joram,[37] B. Jost,[37] N. Jurik,[58] M. Kaballo,[9] S. Kandybei,[42] W. Kanso,[6] M. Karacson,[37] T. M. Karbach,[37] I. R. Kenyon,[44] T. Ketel,[41] B. Khanji,[20] C. Khurewathanakul,[38] S. Klaver,[53] O. Kochebina,[7] I. Komarov,[38] R. F. Koopman,[41] P. Koppenburg,[40] M. Korolev,[31] A. Kozlinskiy,[40] L. Kravchuk,[32] K. Kreplin,[11] M. Kreps,[47] G. Krocker,[11] P. Krokovny,[33] F. Kruse,[9] M. Kucharczyk,[20,25,37,k] V. Kudryavtsev,[33] K. Kurek,[27] T. Kvaratskheliya,[30,37] V. N. La Thi,[38] D. Lacarrere,[37] G. Lafferty,[53] A. Lai,[15] D. Lambert,[49] R. W. Lambert,[41] E. Lanciotti,[37] G. Lanfranchi,[18] C. Langenbruch,[37] T. Latham,[47] C. Lazzeroni,[44] R. Le Gac,[6] J. van Leerdam,[40] J.-P. Lees,[4]

R. Lefèvre,[5] A. Leflat,[31] J. Lefrançois,[7] S. Leo,[22] O. Leroy,[6] T. Lesiak,[25] B. Leverington,[11] Y. Li,[3] M. Liles,[51] R. Lindner,[37] C. Linn,[11] F. Lionetto,[39] B. Liu,[15] G. Liu,[37] S. Lohn,[37] I. Longstaff,[50] J. H. Lopes,[2] N. Lopez-March,[38] P. Lowdon,[39] H. Lu,[3] D. Lucchesi,[21,r] J. Luisier,[38] H. Luo,[49] E. Luppi,[16,f] O. Lupton,[54] F. Machefert,[7] I. V. Machikhiliyan,[30] F. Maciuc,[28] O. Maev,[29,37] S. Malde,[54] G. Manca,[15,e] G. Mancinelli,[6] M. Manzali,[16,f] J. Maratas,[5] U. Marconi,[14] P. Marino,[22,t] R. Märki,[38] J. Marks,[11] G. Martellotti,[24] A. Martens,[8] A. Martín Sánchez,[7] M. Martinelli,[40] D. Martinez Santos,[41] D. Martins Tostes,[2] A. Massafferri,[1] R. Matev,[37] Z. Mathe,[37] C. Matteuzzi,[20] A. Mazurov,[16,37,f] M. McCann,[52] J. McCarthy,[44] A. McNab,[53] R. McNulty,[12] B. McSkelly,[51] B. Meadows,[56,54] F. Meier,[9] M. Meissner,[11] M. Merk,[40] D. A. Milanes,[8] M.-N. Minard,[4] J. Molina Rodriguez,[59] S. Monteil,[5] D. Moran,[53] M. Morandin,[21] P. Morawski,[25] A. Mordà,[6] M. J. Morello,[22,t] R. Mountain,[58] I. Mous,[40] F. Muheim,[49] K. Müller,[39] R. Muresan,[28] B. Muryn,[26] B. Muster,[38] P. Naik,[45] T. Nakada,[38] R. Nandakumar,[48] I. Nasteva,[1] M. Needham,[49] S. Neubert,[37] N. Neufeld,[37] A. D. Nguyen,[38] T. D. Nguyen,[38] C. Nguyen-Mau,[38,q] M. Nicol,[7] V. Niess,[5] R. Niet,[9] N. Nikitin,[31] T. Nikodem,[11] A. Novoselov,[34] A. Oblakowska-Mucha,[26] V. Obraztsov,[34] S. Oggero,[40] S. Ogilvy,[50] O. Okhrimenko,[43] R. Oldeman,[15,e] G. Onderwater,[62] M. Orlandea,[28] J. M. Otalora Goicochea,[2] P. Owen,[52] A. Oyanguren,[35] B. K. Pal,[58] A. Palano,[13,c] M. Palutan,[18] J. Panman,[37] A. Papanestis,[48,37] M. Pappagallo,[50] L. Pappalardo,[16] C. Parkes,[53] C. J. Parkinson,[9] G. Passaleva,[17] G. D. Patel,[51] M. Patel,[52] C. Patrignani,[19,j] C. Pavel-Nicorescu,[28] A. Pazos Alvarez,[36] A. Pearce,[53] A. Pellegrino,[40] G. Penso,[24,m] M. Pepe Altarelli,[37] S. Perazzini,[14,d] E. Perez Trigo,[36] P. Perret,[5] M. Perrin-Terrin,[6] L. Pescatore,[44] E. Pesen,[63] G. Pessina,[20] K. Petridis,[52] A. Petrolini,[19,j] E. Picatoste Olloqui,[35] B. Pietrzyk,[4] T. Pilař,[47] D. Pinci,[24] A. Pistone,[19] S. Playfer,[49] M. Plo Casasus,[36] F. Polci,[8] G. Polok,[25] A. Poluektov,[47,33] E. Polycarpo,[2] A. Popov,[34] D. Popov,[10] B. Popovici,[28] C. Potterat,[35] A. Powell,[54] J. Prisciandaro,[38] A. Pritchard,[51] C. Prouve,[45] V. Pugatch,[43] A. Puig Navarro,[38] G. Punzi,[22,s] W. Qian,[4] B. Rachwal,[25] J. H. Rademacker,[45] B. Rakotomiaramanana,[38] M. Rama,[18] M. S. Rangel,[2] I. Raniuk,[42] N. Rauschmayr,[37] G. Raven,[41] S. Redford,[54] S. Reichert,[53] M. M. Reid,[47] A. C. dos Reis,[1] S. Ricciardi,[48] A. Richards,[52] K. Rinnert,[51] V. Rives Molina,[35] D. A. Roa Romero,[5] P. Robbe,[7] D. A. Roberts,[57] A. B. Rodrigues,[1] E. Rodrigues,[53] P. Rodriguez Perez,[36] S. Roiser,[37] V. Romanovsky,[34] A. Romero Vidal,[36] M. Rotondo,[21] J. Rouvinet,[38] T. Ruf,[37] F. Ruffini,[22] H. Ruiz,[35] P. Ruiz Valls,[35] G. Sabatino,[24,l] J. J. Saborido Silva,[36] N. Sagidova,[29] P. Sail,[50] B. Saitta,[15,e] V. Salustino Guimaraes,[2] B. Sanmartin Sedes,[36] R. Santacesaria,[24] C. Santamarina Rios,[36] E. Santovetti,[23,l] M. Sapunov,[6] A. Sarti,[18] C. Satriano,[24,n] A. Satta,[23] M. Savrie,[16,f] D. Savrina,[30,31] M. Schiller,[41] H. Schindler,[37] M. Schlupp,[9] M. Schmelling,[10] B. Schmidt,[37] O. Schneider,[38] A. Schopper,[37] M.-H. Schune,[7] R. Schwemmer,[37] B. Sciascia,[18] A. Sciubba,[24] M. Seco,[36] A. Semennikov,[30] K. Senderowska,[26] I. Sepp,[52] N. Serra,[39] J. Serrano,[6] P. Seyfert,[11] M. Shapkin,[34] I. Shapoval,[16,42,f] Y. Shcheglov,[29] T. Shears,[51] L. Shekhtman,[33] O. Shevchenko,[42] V. Shevchenko,[61] A. Shires,[9] R. Silva Coutinho,[47] G. Simi,[21] M. Sirendi,[46] N. Skidmore,[45] T. Skwarnicki,[58] N. A. Smith,[51] E. Smith,[54,48] E. Smith,[52] J. Smith,[46] M. Smith,[53] H. Snoek,[40] M. D. Sokoloff,[56] F. J. P. Soler,[50] F. Soomro,[38] D. Souza,[45] B. Souza De Paula,[2] B. Spaan,[9] A. Sparkes,[49] F. Spinella,[22] P. Spradlin,[50] F. Stagni,[37] S. Stahl,[11] O. Steinkamp,[39] S. Stevenson,[54] S. Stoica,[28] S. Stone,[58] B. Storaci,[39] S. Stracka,[22,37] M. Straticiuc,[28] U. Straumann,[39] R. Stroili,[21] V. K. Subbiah,[37] L. Sun,[56] W. Sutcliffe,[52] S. Swientek,[9] V. Syropoulos,[41] M. Szczekowski,[27] P. Szczypka,[38,37] D. Szilard,[2] T. Szumlak,[26] S. T'Jampens,[4] M. Teklishyn,[7] G. Tellarini,[16,f] E. Teodorescu,[28] F. Teubert,[37] C. Thomas,[54] E. Thomas,[37] J. van Tilburg,[11] V. Tisserand,[4] M. Tobin,[38] S. Tolk,[41] L. Tomassetti,[16,f] D. Tonelli,[37] S. Topp-Joergensen,[54] N. Torr,[54] E. Tournefier,[4,52] S. Tourneur,[38] M. T. Tran,[38] M. Tresch,[39] A. Tsaregorodtsev,[6] P. Tsopelas,[40] N. Tuning,[40] M. Ubeda Garcia,[37] A. Ukleja,[27] A. Ustyuzhanin,[61] U. Uwer,[11] V. Vagnoni,[14] G. Valenti,[14] A. Vallier,[7] R. Vazquez Gomez,[18] P. Vazquez Regueiro,[36] C. Vázquez Sierra,[36] S. Vecchi,[16] J. J. Velthuis,[45] M. Veltri,[17,h] G. Veneziano,[38] M. Vesterinen,[11] B. Viaud,[7] D. Vieira,[2] X. Vilasis-Cardona,[35,p] A. Vollhardt,[39] D. Volyanskyy,[10] D. Voong,[45] A. Vorobyev,[29] V. Vorobyev,[33] C. Voß,[60] H. Voss,[10] J. A. de Vries,[40] R. Waldi,[60] C. Wallace,[47] R. Wallace,[12] S. Wandernoth,[11] J. Wang,[58] D. R. Ward,[46] N. K. Watson,[44] A. D. Webber,[53] D. Websdale,[52] M. Whitehead,[47] J. Wicht,[37] J. Wiechczynski,[25] D. Wiedner,[11] L. Wiggers,[40] G. Wilkinson,[54] M. P. Williams,[47,48] M. Williams,[55] F. F. Wilson,[48] J. Wimberley,[57] J. Wishahi,[9] W. Wislicki,[27] M. Witek,[25] G. Wormser,[7] S. A. Wotton,[46] S. Wright,[46] S. Wu,[3] K. Wyllie,[37] Y. Xie,[49,37] Z. Xing,[58] Z. Yang,[3] X. Yuan,[3] O. Yushchenko,[34] M. Zangoli,[14] M. Zavertyaev,[10,b] F. Zhang,[3] L. Zhang,[58] W. C. Zhang,[12] Y. Zhang,[3] A. Zhelezov,[11] A. Zhokhov,[30] L. Zhong[3] and A. Zvyagin[37]

(LHCb Collaboration)

[1]*Centro Brasileiro de Pesquisas Físicas (CBPF), Rio de Janeiro, Brazil*

[2]Universidade Federal do Rio de Janeiro (UFRJ), Rio de Janeiro, Brazil
[3]Center for High Energy Physics, Tsinghua University, Beijing, China
[4]LAPP, Université de Savoie, CNRS/IN2P3, Annecy-Le-Vieux, France
[5]Clermont Université, Université Blaise Pascal, CNRS/IN2P3, LPC, Clermont-Ferrand, France
[6]CPPM, Aix-Marseille Université, CNRS/IN2P3, Marseille, France
[7]LAL, Université Paris-Sud, CNRS/IN2P3, Orsay, France
[8]LPNHE, Université Pierre et Marie Curie, Université Paris Diderot, CNRS/IN2P3, Paris, France
[9]Fakultät Physik, Technische Universität Dortmund, Dortmund, Germany
[10]Max-Planck-Institut für Kernphysik (MPIK), Heidelberg, Germany
[11]Physikalisches Institut, Ruprecht-Karls-Universität Heidelberg, Heidelberg, Germany
[12]School of Physics, University College Dublin, Dublin, Ireland
[13]Sezione INFN di Bari, Bari, Italy
[14]Sezione INFN di Bologna, Bologna, Italy
[15]Sezione INFN di Cagliari, Cagliari, Italy
[16]Sezione INFN di Ferrara, Ferrara, Italy
[17]Sezione INFN di Firenze, Firenze, Italy
[18]Laboratori Nazionali dell'INFN di Frascati, Frascati, Italy
[19]Sezione INFN di Genova, Genova, Italy
[20]Sezione INFN di Milano Bicocca, Milano, Italy
[21]Sezione INFN di Padova, Padova, Italy
[22]Sezione INFN di Pisa, Pisa, Italy
[23]Sezione INFN di Roma Tor Vergata, Roma, Italy
[24]Sezione INFN di Roma La Sapienza, Roma, Italy
[25]Henryk Niewodniczanski Institute of Nuclear Physics Polish Academy of Sciences, Kraków, Poland
[26]Faculty of Physics and Applied Computer Science, AGH—University of Science and Technology, Kraków, Poland
[27]National Center for Nuclear Research (NCBJ), Warsaw, Poland
[28]Horia Hulubei National Institute of Physics and Nuclear Engineering, Bucharest-Magurele, Romania
[29]Petersburg Nuclear Physics Institute (PNPI), Gatchina, Russia
[30]Institute of Theoretical and Experimental Physics (ITEP), Moscow, Russia
[31]Institute of Nuclear Physics, Moscow State University (SINP MSU), Moscow, Russia
[32]Institute for Nuclear Research of the Russian Academy of Sciences (INR RAN), Moscow, Russia
[33]Budker Institute of Nuclear Physics (SB RAS) and Novosibirsk State University, Novosibirsk, Russia
[34]Institute for High Energy Physics (IHEP), Protvino, Russia
[35]Universitat de Barcelona, Barcelona, Spain
[36]Universidad de Santiago de Compostela, Santiago de Compostela, Spain
[37]European Organization for Nuclear Research (CERN), Geneva, Switzerland
[38]Ecole Polytechnique Fédérale de Lausanne (EPFL), Lausanne, Switzerland
[39]Physik-Institut, Universität Zürich, Zürich, Switzerland
[40]Nikhef National Institute for Subatomic Physics, Amsterdam, The Netherlands
[41]Nikhef National Institute for Subatomic Physics and VU University Amsterdam, Amsterdam, The Netherlands
[42]NSC Kharkiv Institute of Physics and Technology (NSC KIPT), Kharkiv, Ukraine
[43]Institute for Nuclear Research of the National Academy of Sciences (KINR), Kyiv, Ukraine
[44]University of Birmingham, Birmingham, United Kingdom
[45]H.H. Wills Physics Laboratory, University of Bristol, Bristol, United Kingdom
[46]Cavendish Laboratory, University of Cambridge, Cambridge, United Kingdom
[47]Department of Physics, University of Warwick, Coventry, United Kingdom
[48]STFC Rutherford Appleton Laboratory, Didcot, United Kingdom
[49]School of Physics and Astronomy, University of Edinburgh, Edinburgh, United Kingdom
[50]School of Physics and Astronomy, University of Glasgow, Glasgow, United Kingdom
[51]Oliver Lodge Laboratory, University of Liverpool, Liverpool, United Kingdom
[52]Imperial College London, London, United Kingdom
[53]School of Physics and Astronomy, University of Manchester, Manchester, United Kingdom
[54]Department of Physics, University of Oxford, Oxford, United Kingdom
[55]Massachusetts Institute of Technology, Cambridge, Massachusetts, USA
[56]University of Cincinnati, Cincinnati, Ohio, USA
[57]University of Maryland, College Park, Maryland, USA
[58]Syracuse University, Syracuse, New York, USA
[59]Pontifícia Universidade Católica do Rio de Janeiro (PUC-Rio), Rio de Janeiro, Brazil, associated with Universidade Federal do Rio de Janeiro (UFRJ), Rio de Janeiro, Brazil

[60]*Institut für Physik, Universität Rostock, Rostock, Germany, associated with Physikalisches Institut, Ruprecht-Karls-Universität Heidelberg, Heidelberg, Germany*
[61]*National Research Centre Kurchatov Institute, Moscow, Russia, associated with Institute of Theoretical and Experimental Physics (ITEP), Moscow, Russia*
[62]*KVI—University of Groningen, Groningen, The Netherlands, associated with Nikhef National Institute for Subatomic Physics, Amsterdam, The Netherlands*
[63]*Celal Bayar University, Manisa, Turkey, associated with European Organization for Nuclear Research (CERN), Geneva, Switzerland*

[a]Also at Universidade Federal do Triângulo Mineiro (UFTM), Uberaba-MG, Brazil.
[b]Also at P.N. Lebedev Physical Institute, Russian Academy of Science (LPI RAS), Moscow, Russia.
[c]Also at Università di Bari, Bari, Italy.
[d]Also at Università di Bologna, Bologna, Italy.
[e]Also at Università di Cagliari, Cagliari, Italy.
[f]Also at Università di Ferrara, Ferrara, Italy.
[g]Also at Università di Firenze, Firenze, Italy.
[h]Also at Università di Urbino, Urbino, Italy.
[i]Also at Università di Modena e Reggio Emilia, Modena, Italy.
[j]Also at Università di Genova, Genova, Italy.
[k]Also at Università di Milano Bicocca, Milano, Italy.
[l]Also at Università di Roma Tor Vergata, Roma, Italy.
[m]Also at Università di Roma La Sapienza, Roma, Italy.
[n]Also at Università della Basilicata, Potenza, Italy.
[o]Also at AGH—University of Science and Technology, Faculty of Computer Science, Electronics and Telecommunications, Kraków, Poland.
[p]Also at LIFAELS, La Salle, Universitat Ramon Llull, Barcelona, Spain.
[q]Also at Hanoi University of Science, Hanoi, Vietnam.
[r]Also at Università di Padova, Padova, Italy.
[s]Also at Università di Pisa, Pisa, Italy.
[t]Also at Scuola Normale Superiore, Pisa, Italy.